Uncertainty in Minimum Cost Multicuts for Image and Motion Segmentation (Supplementary material)

Amirhossein Kardoost[1] **Margret Keuper**[1]

[1]Data and Web Science Group, University of Mannheim, Germany

Abstract

In this supplementary document, we first provide a detailed derivation of the proposed uncertainty measure in terms of the underlying local cut probabilities. Then, we provide additional evaluations of the uncertainties in the context of minimum cost multicuts for motion segmentation when the GAEC heuristic Keuper et al. [2015] is applied as a solver.

1 UNCERTAINTY ESTIMATION

Given an instance of the (lifted) multicut problem and its solution, we employ the probability measures in equations (6) (*MP*) and (7) *(LMP)* of the main paper. We iterate through nodes $v_i \in \{1, \dots, |V|\}$ in vicinity of a cut, i.e. $\exists e \in \mathcal{N}_E(v_i)$ with $e \in E$ and $y_e = 1$. Assuming that v_i belongs to segment A and its neighbour v_j according to E belongs to the segment B, the amount of cost change γ_B is computed in the linear cost function (defined in equations (6) and (7) of the main paper) by moving v_i from cluster A to cluster B as

$$\gamma_B = \sum_{v_j \in \mathcal{N}_{E'}(v_i) \cap A} c_{(v_i,v_j)} - \sum_{v_j \in \mathcal{N}_{E'}(v_i) \cap B} c_{(v_i,v_j)}. \quad (1)$$

Thus, in γ_B, we accumulate all costs of edges from v_i that are not cut in the current decomposition and subtract all costs of edges that are cut in the current decomposition but would not be cut if v_i is moved from A to B. Note that, while the cost change is computed over all edges in E' for lifted graphs, only the uncertainty of nodes with an adjacent cut edge in E can be considered in order to preserve the feasibility of the solution. For each node v_i the number of possible moves depends on the labels of its neighbours $\mathcal{N}_E(v_i)$, and Eq. (6) allows us to assign a cost to any such node-label change. Altogether, we assess the uncertainty of a given node label by the cheapest, i.e. the most likely, possible move

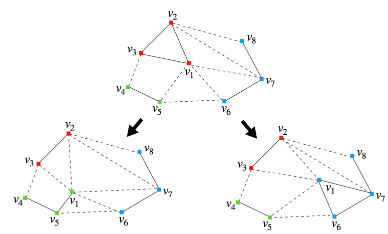

Figure 1: In the current decomposition of the exemplary graph $G = (V, E)$ (top figure), we study the node uncertainties as represented in equation (6). For instance, v_1 is moved from one partition (red label) to the new possible partitions (blue and green labels) and the cost change is estimated. The γ_α represents the cost which minimize the cost among these moves.

$$\gamma_i = \min_B \gamma_B. \quad (2)$$

and set γ_i to ∞ if no move is possible. The minimization in Eq. (2) corresponds to considering the local move of v_i which maximizes

$$\prod_{e=(v_i,v_j), v_j \in A} \frac{p_{\mathcal{Y}_e|\mathcal{X}_e}(1, x_e)}{p_{\mathcal{Y}_e|\mathcal{X}_e}(0, x_e)} \cdot \prod_{e=(v_i,v_j), v_j \in B} \frac{p_{\mathcal{Y}_e|\mathcal{X}_e}(0, x_e)}{p_{\mathcal{Y}_e|\mathcal{X}_e}(1, x_e)}. \quad (3)$$

To produce an uncertainty measure for each node in the graph, we apply the logistic function on (2)

$$\text{uncertainty} = \frac{1}{1 + \exp(-\gamma_i)} \quad (4)$$

as it is the inverse of the logit function used in the cost computation in (8).

In the following we show the expansion of equation (4), by injecting the corresponding values for γ_i. The determine γ_i, the minimum change in the cost is computed among all the possible changes between the clusters for each node $v_i \in V$ (refer to Fig. 1 for an example), such that

$$\text{uncertainty} = \frac{1}{1 + \exp\left(-\min_{B} \gamma_B\right)} \tag{5}$$

where

$$\gamma_B = \sum_{v_j \in \mathcal{N}_{E'}(v_i) \cap A} c_{(v_i,v_j)} - \sum_{v_j \in \mathcal{N}_{E'}(v_i) \cap B} c_{(v_i,v_j)}. \tag{6}$$

The resulting uncertainty measure is thus of the form

$$\begin{aligned}&\text{uncertainty}\\ &= \frac{1}{1 + \exp\left(\sum_{v_j \in \mathcal{N}_{E'}(v_i) \cap B} c_{(v_i,v_j)} - \sum_{v_j \in \mathcal{N}_{E'}(v_i) \cap A} c_{(v_i,v_j)}\right)}.\end{aligned} \tag{7}$$

According to the Bayesian model and the findings in Andres et al. [2012], the costs $c_{(v_i,v_j)}$ for each $e := (v_i, v_j) \in E$ are computed via (refer to the equation (9) in the main paper),

$$\forall e \in E: \quad c_e = \log \frac{p_{\mathcal{Y}_e|\mathcal{X}_e}(0, x_e)}{p_{\mathcal{Y}_e|\mathcal{X}_e}(1, x_e)} + \log \frac{1-\beta}{\beta} \quad . \tag{8}$$

For simplicity and to be compatible with our experiments, we set the value of $\beta = 0.5$ (i.e. we assume an unbiased decomposition), which makes $\log \frac{1-\beta}{\beta} = 0$.

We insert $c(v_i, v_j) = \log \frac{p_{\mathcal{Y}_e|\mathcal{X}_e}(0,x_e)}{p_{\mathcal{Y}_e|\mathcal{X}_e}(1,x_e)}$, $(e = (v_i, v_j))$ into Eq. (7) and denote $v_j \in \mathcal{N}_{E'}(v_i) \cap B$ by e, B where $e = (v_i, v_j), v_j \in B$ and $v_j \in \mathcal{N}_{E'}(v_i) \cap A$ by e, A where $e = (v_i, v_j), v_j \in A$, and get

$$\begin{aligned}
&\text{uncertainty}\\
&= \frac{1}{1 + \exp\left(\sum_{e,B} \log \frac{p_{\mathcal{Y}_e|\mathcal{X}_e}(0, x_e)}{p_{\mathcal{Y}_e|\mathcal{X}_e}(1, x_e)} - \sum_{e,A} \log \frac{p_{\mathcal{Y}_e|\mathcal{X}_e}(0, x_e)}{p_{\mathcal{Y}_e|\mathcal{X}_e}(1, x_e)}\right)}\\
&= \frac{1}{1 + \exp\left(\log \prod_{e,B} \frac{p_{\mathcal{Y}_e|\mathcal{X}_e}(0, x_e)}{p_{\mathcal{Y}_e|\mathcal{X}_e}(1, x_e)} - \log \prod_{e,A} \frac{p_{\mathcal{Y}_e|\mathcal{X}_e}(0, x_e)}{p_{\mathcal{Y}_e|\mathcal{X}_e}(1, x_e)}\right)}\\
&= \frac{1}{1 + \exp\left(\log \prod_{e,B} \frac{p_{\mathcal{Y}_e|\mathcal{X}_e}(0, x_e)}{p_{\mathcal{Y}_e|\mathcal{X}_e}(1, x_e)} + \log \prod_{e,A} \frac{p_{\mathcal{Y}_e|\mathcal{X}_e}(1, x_e)}{p_{\mathcal{Y}_e|\mathcal{X}_e}(0, x_e)}\right)}\\
&= \frac{1}{1 + \exp\left(\log\left(\prod_{e,B} \frac{p_{\mathcal{Y}_e|\mathcal{X}_e}(0, x_e)}{p_{\mathcal{Y}_e|\mathcal{X}_e}(1, x_e)} \cdot \prod_{e,A} \frac{p_{\mathcal{Y}_e|\mathcal{X}_e}(1, x_e)}{p_{\mathcal{Y}_e|\mathcal{X}_e}(0, x_e)}\right)\right)}\\
&= \frac{1}{1 + \left(\prod_{e,B} \frac{p_{\mathcal{Y}_e|\mathcal{X}_e}(0, x_e)}{p_{\mathcal{Y}_e|\mathcal{X}_e}(1, x_e)} \cdot \prod_{e,A} \frac{p_{\mathcal{Y}_e|\mathcal{X}_e}(1, x_e)}{p_{\mathcal{Y}_e|\mathcal{X}_e}(0, x_e)}\right)}\\
&= \frac{1}{1 + \left(\frac{\prod_{e,B} p_{\mathcal{Y}_e|\mathcal{X}_e}(0, x_e)}{\prod_{e,B} p_{\mathcal{Y}_e|\mathcal{X}_e}(1, x_e)} \cdot \frac{\prod_{e,A} p_{\mathcal{Y}_e|\mathcal{X}_e}(1, x_e)}{\prod_{e,A} p_{\mathcal{Y}_e|\mathcal{X}_e}(0, x_e)}\right)}
\end{aligned} \tag{9}$$

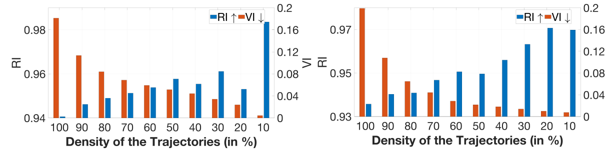

Figure 2: Study on the trajectory uncertainty on the GAEC Keuper et al. [2015] solver. The experiment relates to the Variation of Information (VI) and Rand Index (RI) on the train (left) and test (right) set of FBMS_{59} Ochs et al. [2014].

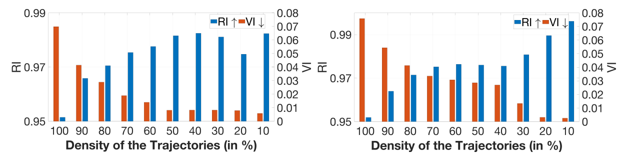

Figure 3: Study on the trajectory uncertainty on the GAEC Keuper et al. [2015] solver. The experiment relates to the Variation of Information (VI) and Rand Index (RI) on the train (left) and validation (right) set of DAVIS_{2016} Perazzi et al. [2016].

Note that in the denominator, we have exactly 1 + the term from Equation (12) in the main paper. With a slight reformulation, we get

$$= \frac{\prod_{e,A} p_{\mathcal{Y}_e|\mathcal{X}_e}(0, x_e) \cdot \prod_{e,B} p_{\mathcal{Y}_e|\mathcal{X}_e}(1, x_e)}{\prod_{e,A} p_{\mathcal{Y}_e|\mathcal{X}_e}(0, x_e) \cdot \prod_{e,B} p_{\mathcal{Y}_e|\mathcal{X}_e}(1, x_e) + \prod_{e,B} p_{\mathcal{Y}_e|\mathcal{X}_e}(0, x_e) \cdot \prod_{e,A} p_{\mathcal{Y}_e|\mathcal{X}_e}(1, x_e)} \tag{10}$$

or by a simplified notation $p_{\mathcal{Y}_e|\mathcal{X}_e}(1, x_e) =: p_c$ for *cut* probabilities and $p_{\mathcal{Y}_e|\mathcal{X}_e}(0, x_e) =: p_j$ for *join* probabilities.

$$\text{uncertainty} = \frac{\prod_{e,B} p_c \prod_{e,A} p_j}{\prod_{e,B} p_c \prod_{e,A} p_j + \prod_{e,B} p_j \prod_{e,A} p_c} \quad (11)$$

where the nominator is exactly the product of the local probabilities for the observed solution at node v_i (compare Eq. (6) in the main paper) and the denominator sums trivially to one in the case of $|\mathcal{N}_{E'}(v_i)| = 1$.

2 UNCERTAINTY ON MINIMUM COST MULTICUT SOLUTIONS FROM GAEC

In Figures 2 and 3, we provide an additional evaluation of the proposed uncertainty measure in the motion segmentation setting. Specifically, we compute solutions for the same motion segmentation problem instances as used in the main paper on the FBMS_{59} and DAVIS_{2016} datasets. While the main paper evaluates using the widely employed high quality solutions from the KLj heuristic, we here additionally assess uncertainties on a faster, lower quality solver, GAEC Keuper et al. [2015]. It can be seen that the sparsification plots behave as expected. The VI decreases as the segmentation becomes sparser and the RI increases. However, it can be seen that for the poorer segmentation results, the RI does not increase as monotonically as this was the case for KLj. Specifically when considering the high sparsity regime, the RI metric becomes brittle, indicating that entire labels might have been removed from the solution.

References

B. Andres, T. Kröger, K. L. Briggman, W. Denk, N. Korogod, G. Knott, U. Köthe, and F. A. Hamprecht. Globally optimal closed-surface segmentation for connectomics. In *ECCV*, 2012.

M. Keuper, E. Levinkov, N. Bonneel, G. Lavoué, T. Brox, and B. Andres. Efficient decomposition of image and mesh graphs by lifted multicuts. *ICCV*, pages 1751–1759, 2015.

P. Ochs, J. Malik, and T. Brox. Segmentation of moving objects by long term video analysis. *IEEE TPAMI*, 36 (6):1187 – 1200, Jun 2014.

F. Perazzi, J. Pont-Tuset, B. McWilliams, L. Van Gool, M. Gross, and A. Sorkine-Hornung. A benchmark dataset and evaluation methodology for video object segmentation. pages 724–732, 06 2016.